Gaseous Diffusion in the Transition Pressure Range

T. E. MISTLER, G. R. CORRELL, and J. O. MINGLE

Kansas State University, Manhattan, Kansas

Measurements of the effective self-diffusion coefficients for carbon dioxide and methane were performed in the transition pressure range. The experiments utilized carbon-14 tagged gases and semiconductor radiation detectors in a transient type of experiment. A detailed analysis of the errors associated with the experiments indicated that the accuracy of the measurements was near 5%. The results verify that the additive resistance law is valid for the representation in the transition range. The unknown effects of surface diffusion make the values to be employed in this law subject to review. As an example one surface diffusion model is considered.

The role of mass transport is assuming a significantly greater share of the developmental work necessary to successfully design and operate a system containing composition gradients. Since mass transport is directly dependent upon values for diffusion coefficients, the experimental and theoretical efforts in this field have been directed toward this goal. Several investigators such as Bird (*1*) have presented complicated solutions to diffusion problems, but in all cases the results are unusable if realistic numerical values for the diffusion coefficients are not available.

The theory of diffusion can be arbitrarily broken down into three main areas. These are (a) normal gaseous diffusion where the mean free path of the molecules is short enough so that only intermolecular collisions are important, but long enough so that short-ranged intermolecular forces are small, (b) diffusion in liquid and highly compressed media where the short-ranged forces are significant, and (c) Knudsen diffusion where the mean free path of the molecules is significantly greater than a dimension of the constraints of the system so the intermolecular collisions represent a negligible contribution to the total transfer. At present the theory for areas (a) and (c) are generally available, while area (b) is being explored currently by theorists. However, extensive experimental data are missing in nearly all the areas. In addition, neither the theory nor the experimental data are present for the transition ranges between the various types of diffusion where two of the areas are significantly contributing to the total result. The purpose of this experimental study is to measure the transition range diffusion coefficient of gases (that is, diffusion where areas (a) and (c) are both significant) in a modified Ney-Armistead diffusion cell by using a semiconductor radiation detector and carbon-14 tagged isotopes.

TRANSITION RANGE DIFFUSION

The transition range of diffusion between normal gaseous diffusion and Knudsen diffusion has generally been correlated by evaluating an effective diffusion coefficient, D_e. Since from general kinetic theory (*2*), the bulk diffusion coefficient is inversely proportional to pressure whereas the Knudsen diffusion coefficient is independent of pressure, transition range diffusion can be produced by the selective regulation of pressure when a fixed size system is utilized. In this work, it is found convenient to employ a capillary tube of approximately 0.1 cm. in diameter and operate in a pressure range of 40 to 500 μ of mercury. Thus the effective diffusion coefficient is measured as a function of system pressure.

Normal gaseous diffusion has been correlated to various degrees of accuracy, but in particular in the low density regions the theoretical expression given by the Chapman and Enskog theory (*3*) and summarized by Hirschfelder (*2*) is utilized:

$$D_{11} = 2.628(10^{-3})\ [T^3/m]^{1/2}\ [p\sigma^2_{11}\Omega_{11}(T^*)]^{-1} \quad \text{(sq.cm./sec.)} \qquad (1)$$

where the equation has been written for self-diffusion. In the Knudsen range the theory has been summarized by Present (*4*) who gives the ideal result for a circular pore in the form

$$D_k = 9701\ r\,[T/m]^{1/2} \quad \text{(sq.cm./sec.)} \qquad (2)$$

For the transition range Bosanquet (*5*) has proposed an additive resistance law

$$1/D_e = 1/D_k + 1/D_{11} \qquad (3)$$

which states that the resistance to transport is the sum of the resistance caused by wall collisions and by intermolecular collisions. Wheeler (*6*) has proposed an empirical combination as

$$D_e = D_{11}\,[1 - \exp(-D_k/D_{11})] \qquad (4)$$

This equation has been deduced from intuitive reasoning, but it does give a smooth transition between the two extremes. It is noted that in the transition range of pressure the combining rules of Bosanquet and Wheeler are considerably different.

Other theories of diffusion in the transition pressure range are summarized by Mistler (*7*); however in this study only Bosanquet's and Wheeler's expression are employed for comparison with experiment. This is especially valid for self-diffusion as many more complex theories reduce to that of Bosanquet for this simple case.

INTERPRETATION OF EXPERIMENTS

Generally two methods are applied to measure diffusion coefficients: 1. a steady state type of experiment in which flow streams of different compositions pass on opposite sides of a barrier through which diffusion occurs, or 2. a

---

T. E. Mistler is with Westinghouse Atomic Power Divisions, Pittsburgh, Pennsylvania, and G. R. Correll is with Douglas United Nuclear, Inc., Richland, Washington.

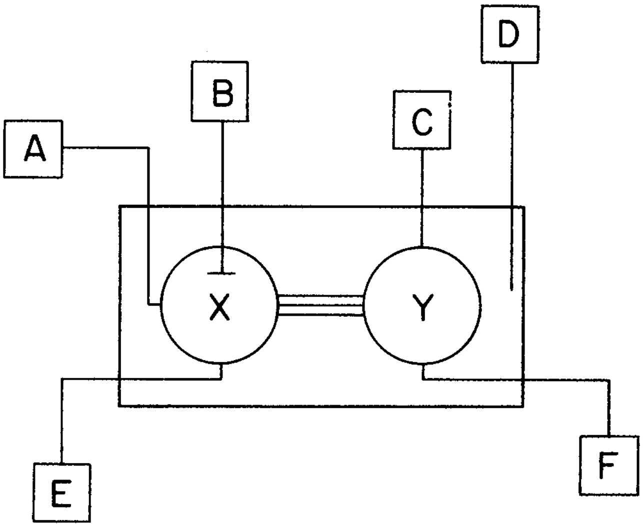

Fig. 1. Schematic diagram of diffusion cell. Components are: A. $C^{14}H_4$ charging system. B. Electronic counting system. C. Vacuum measurement system. D. Constant temperature control system. E. Vacuum producing system. F. Methane charging system. X. Flask 1. Y. Flask 2.

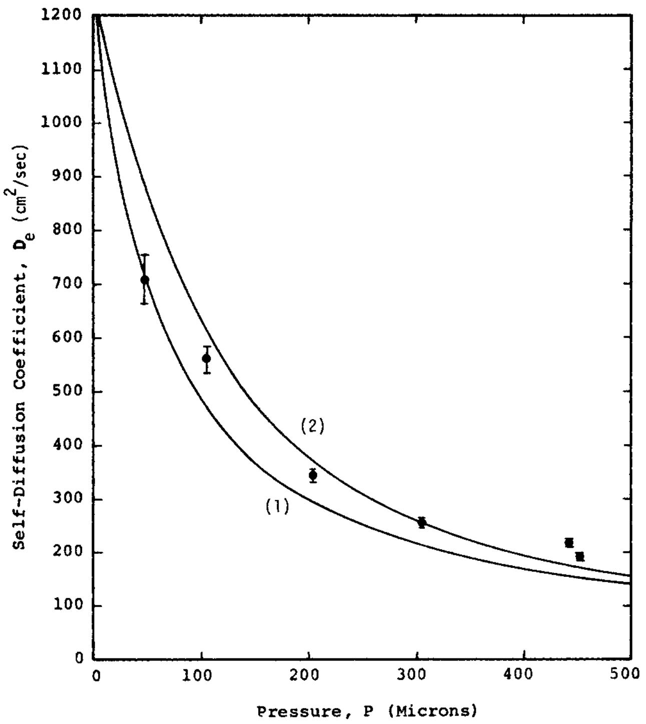

Fig. 2. Comparison between experimental and theoretical self-diffusion coefficients for carbon dioxide. Curve (1) = Equation (3), curve (2) = Equation (4).

transient experiment whereby diffusion eliminates a zero-time concentration difference between two parts of a closed batch system. Method 1 requires a large amount of material as well as precise flow control. The difficulty with method 2 has been the measurement of concentration as a function of time, but the advances of radioisotope detection and availability have made their use very feasible for this type of experiment. In particular, the employment of semiconductor radiation detectors has made the internally isolated detection of tagged materials very plausible. In this study method 2 is employed to measure self-diffusion of carbon dioxide and methane by utilizing a modified Ney-Armistead (8) cell, sometimes referred to as the *Loschmidt method* (19). Mistler (7) summarizes the types of experimental cells that have been utilized for diffusion measurements as well as describing the current cells in use. Figure 1 is a schematic of the cell and its associated system.

By using the Ney-Armistead apparatus the partial differential equation for one-dimensional diffusion through the capillary tube is

$$\frac{\partial c(z,t)}{\partial t} = D_e \frac{\partial^2 c(z,t)}{\partial z^2} \tag{5}$$

where the assumption of Fick's law (2) is valid since the tagged material is present in small concentrations. The boundary conditions are

$$c(z,0) = C_1 \tag{6}$$

$$c(0,t) = C_0 - V_1^{-1} \int_0^t \left[-D_e(\pi r^2) \frac{\partial c(0,t)}{\partial z} \right] dt \tag{7}$$

$$c(L,t) = C_1 + V_2^{-1} \int_0^t \left[-D_e(\pi r^2) \frac{\partial c(L,t)}{\partial z} \right] dt \tag{8}$$

Equation (6) indicates that at zero time the capillary tube contains a concentration of the tagged isotope of level C_1 where $C_1 < C_0$. Equation (7) shows that the composition of the tagged isotope in flask one is the original amount less the total amount leaving flask one by diffusion into the capillary tube. The boundary condition of Equation (8) states that the composition under the assumption of uniform mixing represents the cumulative amount of material diffusing from the tube plus the initial value. The complete solution to Equation (5) in dimensionless variables is

$$\begin{aligned} x(\xi,\tau) = {} & [\beta + \alpha x_1(1+\beta)]\,[\alpha+\beta+\alpha\beta]^{-1} \\ & - [1 - x_1] \sum_{n=1}^{\infty} [\exp(-\lambda_n^2\tau)]\quad [\lambda_n \cos\lambda_n + \beta \sin\lambda_n] \\ & [\alpha \cos(\lambda_n\xi) - \lambda_n \sin(\lambda_n\xi)]\,\{\lambda_n^2\,[(2\lambda_n)^{-1} \\ & \cdot (\cos\lambda_n)\,(\alpha+\beta+\alpha\beta-\lambda_n^2) \\ & - (\sin\lambda_n)\,(1 + (\alpha+\beta)/2)]\}^{-1} \end{aligned} \tag{9}$$

where λ_n are the nonzero positive roots of

$$\tan\lambda_n = \lambda_n(\alpha+\beta)\,[\lambda_n^2 - \alpha\beta]^{-1} \tag{10}$$

The concentration vs. time data are obtained from the multiscaler mode of a multichannel analyzer output, which represents the number of particles detected by the surface-barrier detector within a specified time increment at various times after the capillary valve has been opened. Correll (9) describes in detail the properties of these detectors that make their use advantageous for Method 2 experiments.

During the charging phase of the experiment it is very difficult not to produce a pressure gradient between the two flasks. The degree to which this pressure differential could be eliminated and its effect upon the subsequent diffusion process is analyzed in the discussion section. However, during this equilization some tracer material entered the second flask and the capillary tube. This along with some leakage through the capillary valve produced an initial concentration, C_1, in the diffusion tube. For a valid experimental run though it was necessary to require that $C_1 << C_0$; thus in practice x_1 was generally in the range of a few hundredths. A sample set of normalized concentration vs. time data for methane for which D_e is 614 ± 14 sq.cm./sec. is given in Table 1.

Experimental diffusion coefficients are determined by utilizing the technique of nonlinear least squares analysis to give a best fit of the mathematical model to the normalized data. Thus the fitting equation is

$$\sum_{i=1}^{N} [\underline{x}(0, \tau_i) - x(0, \tau_i)] \frac{\partial x(0, \tau_i)}{\partial \tau} = 0 \quad (11)$$

where $\underline{x}$ represents the experimental data and the partial derivative is evaluated from Equation (9).

Errors incurred in the experimental measurements of count rate of the carbon-14 tagged gas caused considerable scatter of the data about the mathematical curve representing the diffusion process. A normal distribution is assumed for errors in measurement of the count rate while time measurements are assumed to have negligible error. Confidence limits on the individual diffusion coefficients are based upon the residues of the curve from which each D_e is determined. Utilizing the theory of nonlinear least squares analysis the variance of the effective diffusion coefficient becomes

$$\sigma^2_{D_e}(N) = \sigma_x^2 \left\{ \sum_{i=1}^{N} \left[\frac{L^2}{t} \frac{\partial x(0, \tau_i)}{\partial D_e} \right]^2 \right\}^{-1} \quad (12)$$

An estimate for σ_x^2 can be obtained from Brownlee (*10*) and is based upon the residuals between the least squares fit and the actual data. This is

$$\sigma_x^2 = [N-1]^{-1} \sum_{i=1}^{N} [\underline{x}(0, \tau_i) - x(0, \tau_i)]^2 \quad (13)$$

Equation (12) represents the variance caused by the uncertainty in the data fit and is a function of the number of data points. The uncertainty in the analysis because of the error in pressure measurement represent an additional variance to the diffusion coefficient. Rather than overly complicate the analysis with a two variable variance model, the effect of pressure error can be estimated by accepting Bosanquet's relationship. Thus using Equations (1) and (3) and writing

$$D_{11} = D_{11}^{(1)}/p \quad (14)$$

where $D_{11}^{(1)}$ is the self diffusion coefficient at 1 atm. pressure and p is in atmospheres. The effective diffusion coefficient is then

$$\begin{aligned} D_e &= [1/D_k + p/D_{11}^{(1)}]^{-1} \\ &= D_k D_{11}^{(1)} [D_{11}^{(1)} + D_k p]^{-1} \quad (15) \end{aligned}$$

so that the variance then becomes

$$\sigma^2_{D_e}(p) = \left[\frac{\partial D_e}{\partial p} \right]^2 \sigma_p^2 = [D_e^2/D_{11}^{(1)}]^2 \sigma_p^2 \quad (16)$$

Thus the total variance is

$$\sigma^2_{D_e} = \sigma^2_{D_e}(N) + \sigma^2_{D_e}(p) \quad (17)$$

The value of σ_p^2 is estimated by fitting the calibration data for the pressure measurement gauges by polynomial approximations and then estimating the variance of the fit at the desired pressure level.

Generally the $\sigma^2_{D_e}(p)$ values are small compared to the $\sigma^2_{D_e}(N)$ result as can be inferred from the Table 1 data where $\sigma_{D_e}(p)$ is 2 sq.cm./sec. while $\sigma_{D_e}(N)$ is 12 sq.cm./sec.

Experimentally determined values of the self-diffusion coefficient for carbon dioxide in the transition pressure range at 20°C. are presented in Table 2* and Figure 2. Corresponding values for methane are shown in Table 3* and Figure 3. The results for each gas has been compared with theoretical values predicted by the relationships of Bosanquet and Wheeler, Equations (3) and (4) respectively. Values of D_{11} in the theoretical calculations are derived from the theory of Chapman and Cowling at 760 mm. pressure and 20°C. For carbon dioxide, the theoretical self-diffusion coefficient under these conditions is 0.102 sq.cm./sec.; for methane it is 0.203 sq.cm./sec. The Knudsen coefficients are found from Equation (2) for the 0.1026 cm. I.D. capillary tube and for 20°C. They are 1,284 and 2,127 sq.cm./sec. for carbon dioxide and methane respectively. The reported values of D_e are calculated by using experimental values for the diffusion coefficient of the tracer gas in the natural gas and correcting these for carbon-14 diffusion. This Hutchinson (*11*) factor is shown by

$$D_{11} = [2m_2/(m_1 + m_2)]^{1/2} D_{12} \quad (18)$$

as can be derived from the inverse square root relationship of the diffusion coefficient with the mass of the diffusing molecule as is shown by Equations (1) and (2). For $C^{14}O_2$ in carbon dioxide the correction factor is 1.011 while for $C^{14}H_4$ in methane it is 1.029.

The deviation reported for each experimental diffusion coefficient is the standard deviation which corresponds to 67% confidence limits. This deviation is a measure of the accuracy of the least squares fit of the data and of the

TABLE 1. SAMPLE SET OF COUNT RATES VS. TIME DATA TAKEN FROM THE ANALYZER OUTPUT

Mean Time* (sec.)	Counts Channel	Mean Time* (sec.)	Counts Channel	Mean Time* (sec.)	Counts Channel
0	1,693	578	1,181	1,165	1,048
29	1,654	597	1,147	1,185	970
49	1,667	617	1,209	1,204	1,006
69	1,652	636	1,177	1,224	1,004
88	1,561	656	1,167	1,244	1,008
108	1,516	676	1,111	1,263	1,000
127	1,490	695	1,209	1,283	955
147	1,483	715	1,166	1,302	1,000
166	1,562	734	1,139	1,322	970
186	1,547	754	1,106	1,341	925
206	1,505	774	1,069	1,361	993
225	1,398	793	1,097	1,381	973
245	1,392	813	1,061	1,400	973
246	1,378	832	1,096	1,420	976
284	1,405	852	1,054	1,439	1,011
304	1,246	871	1,112	1,459	949
323	1,481	891	1,057	1,479	947
343	1,361	911	1,077	1,498	956
362	1,316	930	1,148	1,518	918
382	1,272	950	1,036	1,537	1,003
401	1,289	969	1,010	1,557	976
421	1,247	989	1,057	1,576	887
441	1,288	1,028	1,059	1,596	920
460	1,297	1,048	1,042	1,616	913
480	1,210	1,067	1,032	1,635	955
499	1,266	1,087	1,048	1,655	974
519	1,202	1,106	1,021	1,674	957
539	1,156	1,126	1,125	1,694	941
558	1,220	1,148	951	1,714	896
				1,733	967

$p = 203\ \mu$ Hg

Initial pressure difference = $-2\ \mu$ Hg.

D_e before pressure-induced flow correction = 614 sq.cm./sec.

Deviation arising only from least squares analysis = 12 sq.cm./sec.

Combined deviation caused by least squares and uncertainty of pressure measurement = 14 sq.cm./sec.

D_e after correction for pressure-induced flow = 617 sq.cm./sec.

* The measured time increment was 19.583 sec.; all the times above have been rounded to the nearest second.

---

* Tabular material has been deposited as document 00568 with the ASIS National Auxiliary Publications Service, c/o CCM Information Sciences, microfiche or $3.00 for photocopies.

uncertainty of pressure measurements. For the carbon dioxide data the error represented by these deviations ranges from 6.4% for the measurement at 46 μ to 2.7% for the measurement at 442 μ. The improved precision in these new measurements can be compared with the previous data of Mistler (*7*) where in the low pressure ranges an abnormally large value of the initial composition of tagged material, C_1, is occurring. For methane the percentage deviations range generally from 2 to 3% with only an occasional instance as high as 5.5% at pressures of approximately 50 μ. Pressure control and measurement also were responsible for some error in the determinations, which is represented by $\sigma_D(p)$ and is included in the reported standard deviation. This uncertainty in pressure measurement generally accounted for less than 30% of the total deviation.

The presence of a pressure gradient between the two flasks would of course result in an erroneous measurement of the diffusion coefficient. By use of pressure gauges in both flasks this problem is essentially eliminated. An analysis of the error associated with a pressure gradient is determined from the theory of Wakao, Otani, and Smith (*16*) who analyzed the combined diffusion flow case. From their theory an approximate expression for the time dependence of the pressure gradient between the two flasks can be obtained as

$$\Delta P(t) = \Delta P_0 e^{-k_1 t} \qquad (19)$$

where k_1 is an experimentally measured relaxation constant that proved to be a function of the total pressure of the system. The half-life associated with k_1 varied from 330 sec. at 50 μ pressure down to 70 sec. at 500μ total pressure. For any given run through k_1 was assumed to be constant. Utilizing Equation (19) the expression for the flux change because of pressure-induced flow is

$$\Delta x = k_2 e^{-k_1 t} \qquad (20)$$

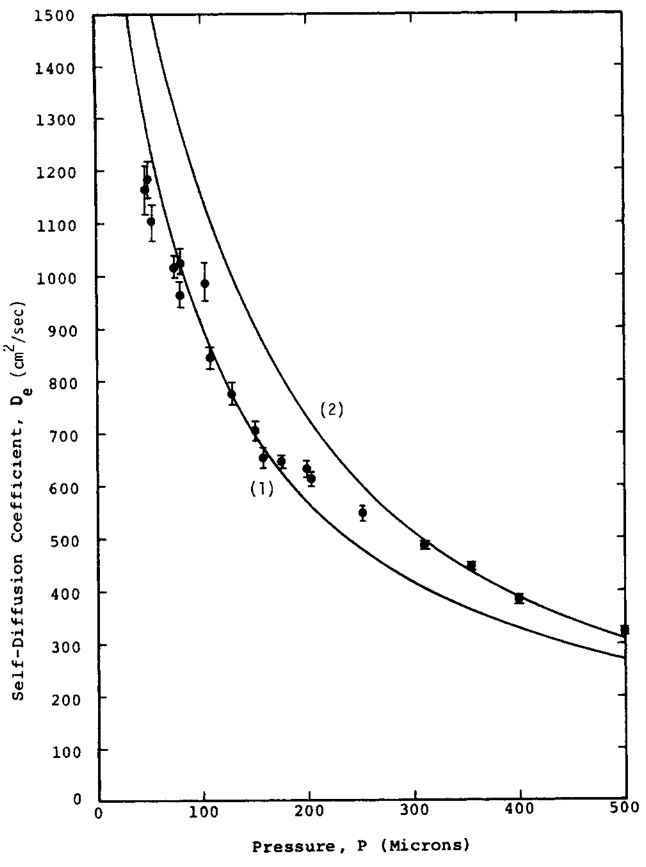

Fig. 3. Comparison between experimental and theoretical self-diffusion coefficients for methane. Curve (1) = Equation (3), curve (2) = Equation (4).

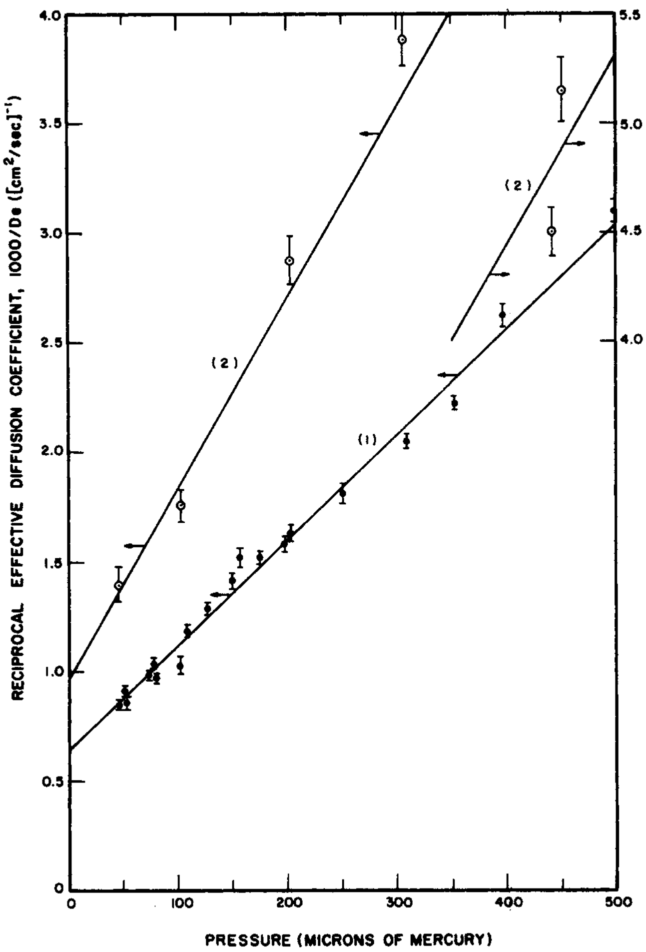

Fig. 4. Additive resistance law graph for experimental data. Curve (1) = Equation (25), curve (2) = Equation (26).

where k_2 is a constant found from the expression of Wakao (*16*).

By correcting representative runs by the above correction and re-evaluating the diffusion coefficient produced values differing by less than 1% from the previous results. The correction to the data of Table 1 changed the effective diffusion coefficient from 614 to 617 sq.cm./sec., a correction of less than ½%.

Mistler (*17*) has summarized a study of errors caused by inaccuracies in the measurement of system parameters and in general these errors are found to be small in comparison with the counting error associated with the reported standard deviation.

Another possible source of error is the Rayleigh (*18*) end correction which is used for determining the effective tube length. Although this is the accepted method of correction, it does not allow for expected changes in the diffusion length as Knudsen diffusion becomes predominant; however the long tube length is expected to minimize this error. Presently no relationship has been accepted for the change in effective tube length as a function of pressure.

From the experimental measurements of the effective diffusion coefficient as shown in Figures 2 and 3 for carbon dioxide and methane respectively, it is noted that as the pressure increases, the experimental result is larger than that predicted by the Bosanquet relationship utilizing theoretical values for the Knudsen and bulk diffusion coefficients. The correlation of Wheeler is also shown for comparison.

TABLE 4. COMPARISON OF EXPERIMENTAL AND THEORETICAL DIFFUSION COEFFICIENTS ASSUMING BOSANQUET'S LAW

	Diffusion Coefficient (sq.cm./sec.) Experimental Equation (21)	Theoretical	Surface Equation (27)
Carbon dioxide			
D_k	1,047 ± 94	1,284	5,674 ± 2,747
$D_{11}^{(1)}$	0.151 ± 0.006	0.102	−0.316 ± 0.027
methane			
D_k	1,580 ± 30	2,127	6,142 ± 448
$D_{11}^{(1)}$	0.274 ± 0.004	0.203	−0.786 ± 0.033

If the assumption of the additive resistance law is utilized, then Equation (3) can be written

$$1/D_e = 1/D_k + p/(D_{11}p) \qquad (21)$$

Since $D_{11}p$ is a constant, this equation relates $1/D_e$ to pressure as a straight line with an intercept of $1/D_k$ and a slope of $1/(D_{11}p)$. The experimental data plotted in this form are shown in Figure 4. In order to employ a standard least squares analysis with weighting function (*10*), it is necessary to evaluate the variance of the data in the form required by Equation (21); therefore since $\sigma_{D_e} << D_e$

$$[D_e \pm \sigma_{D_e}]^{-1} \cong D_e^{-1} + \sigma_{D_e}/D_e^2 \qquad (22)$$

and the weighting factor is

$$W = \sigma_{1/D_e}{}^{-2} = [D_e^2/\sigma_{D_e}]^2 \qquad (23)$$

These results are shown in Table 4.

These values differ from the theoretical results by from 11 to 48%; however in each case the experimental Knudsen diffusion coefficient is low and the experimental bulk diffusion coefficient is high. This trend for experimental bulk diffusion coefficients is common for the results reported by Mathur and Thodos (*20*) in their compilation are 0.117 sq.cm./sec. for carbon dioxide and 0.234 sq.cm./sec. for methane which are both higher than the theoretical value. In fact a more realistic model for normal diffusion where more than binary collisions are allowed would predict a higher value than the simple binary model (*2*).

A statistical F-test (*10*) performed on the correlations of Figure 4 definitely shows that the results fit a straight line best. This could also have been inferred from the standard deviations of Table 4 for these experimental results based on Equation (21). Thus it would appear that Bosanquet's additive resistance law is valid. The question of the values to employ in the relationship still remains though.

Another unknown factor is the effect of surface diffusion on the experimental results. The theory of surface diffusion is incomplete at present, with some summary discussions presented by Reynolds and Richley (*12*, *13*), Clausing (*14*), and Hill (*15*). If it is hypothesized that an effective surface diffusion coefficient would obey the same physical additive resistance law then

$$1/D_e = 1/D_k + 1/D_{11} + 1/D_s \qquad (24)$$

The results of Figure 4 put in this form and utilizing the theoretical results for the Knudsen and bulk diffusion coefficients produces

For methane:

$$10^3/D_e = 1/2.127 + 1/6.142 + [p/760]\,[1/0.203 - 1/0.786] \qquad (25)$$

For carbon dioxide:

$$10^3/D_e = 1/1.284 + 1/5.674 + [p/760]\,[1/0.102 - 1/0.316] \qquad (26)$$

where p is in microns of mercury. Therefore the surface diffusion coefficient can be written as

$$1/D_s = 1/D_{ks} + p/(D_{11s}p) \qquad (27)$$

with values and their standard deviations as shown in Table 4.

These results indicate that in the Knudsen range surface diffusion is very rapid and that the normal Knudsen diffusion would be the dominant factor. However the effect of pressure is negative and the crossover is near 50 μ of mercury pressure for both gases so that measurement made near this point should show little surface diffusion effects. This is only valid for a temperature of 20°C. and at other temperatures a different crossover point would be found.

Because of molecular polarity effects the surface diffusion trends for carbon dioxide would be expected to be greater than methane. This is verified by the experimental results as the slope of the pressure vs. reciprocal surface diffusion coefficient curve is more negative for carbon dioxide than for methane.

CONCLUSIONS

The discussion and results presented above have shown the advantages of this experimental apparatus for measuring diffusion coefficients. The feasibility of using a semiconductor detector in a modified Ney-Armisted diffusion cell to measure diffusion coefficients has been demonstrated and accurate transition range diffusion coefficients for carbon dioxide and methane were measured. In general the theory of Bosanquet was found to represent the data to an accuracy of a few percent. The question remains as to what the effect of surface diffusion is on diffusion measurements in general.

ACKNOWLEDGMENT

This work was supported by the Kansas State University Experiment Station and the Petroleum Research Fund of the American Chemical Society under Grant 1622-A2.

NOTATION

$c(z, t)$ = concentration of tagged material at position z in the tube at time, t, atoms/cc.
C_0 = concentration of tagged material in Flask 1 at zero time, atoms/cc.
C_1 = base tube concentration, atoms/cc.
D = diffusion coefficient (see subscripts), sq.cm./sec.
k_i = constant
L = length of capillary tube, cm.
m = molecular weight of diffusing specie
N = number of data points
p = pressure, atm.
r = radius of capillary tube, cm.
t = time, sec.
T = temperature, °K.
T^* = kT/ϵ, molecular parameter, (2)
V_i = volume of Flask i (cc.)
W = weighting factor
$x(\xi, \tau)$ = $c(z, t)/C_0$
x_1 = C_1/C_0
$\underline{x}(0, \tau)$ = dimensionless experimental concentration in Flask 1 at reduced time, τ
z = distance variable along capillary tube, cm.

Greek Symbols

α = $\pi r^2 L/V_1$
β = $\pi r^2 L/V_2$
λ_n = nth eigenvalue
ξ = z/L

σ = molecular interaction parameter, (2)
σ_i = standard deviation of i
τ = tD_e/L^2
Ω = molecular potential energy parameter, (2)

Subscripts

1 = species one
2 = species two
e = effective
k = Knudsen
s = surface

LITERATURE CITED

1. Bird, R. B., and H. W. Heu, *AIChE J.*, **6**, 516 (1960).
2. Hirschfelder, J. O., et. al., "Molecular Theory of Gases and Liquids," John Wiley, New York (1954).
3. Chapman, S., and T. G. Cowling, "The Mathematical Theory of Non-Uniform Gases," Cambridge University Press, Cambridge, (1960).
4. Present, R. D., "The Kinetic Theory of Gases," McGraw-Hill, New York (1958).
5. Bosanquet, C. H., *British TA Rept., BR-507* (Sept., 1944).
6. Wheeler, A., *Catalysis*, **2**, 105 (1955).
7. Mistler, T. E., and J. O. Mingle, *Chem. Eng. Progr. Symposium* Ser., No. 68, **62**, 95 (1966).
8. Ney, E. P., and F. C. Armisted, *Phys. Rev.*, **71**, 14 (1947).
9. Correll, G. R., MS thesis, Kansas State Univ., Manhattan (1967).
10. Brownlee, K. A., "Statistical Theory and Methodology in Science and Engineering," 2nd Ed., John Wiley, New York (1965).
11. Hutchinson, F., *J. Chem. Phys.*, **17**, 1081, 1949.
12. Reynolds, T. W., and E. A. Richley, *Nat. Aeron. Space Admin. TN D-3225*, (1966).
13. *Ibid., TR R-255*, (1967).
14. Clausing, P., *Ann. Phys.*, **12**, 961 (1932).
15. Hill, T. L., *J. Chem. Phys.*, **25**, 730 (1956).
16. Wakao, N., et. al., *AIChE J.*, **11**, 435 (1965).
17. Mistler, T. E., MS thesis, Kansas State Univ., Manhattan (1966).
18. Rayleigh, Lord, "Theory of Sound," Vol. 2, Dover Publ., New York (1945).
19. Loschmidt, J., *Sitzb. Akad. Wiss. Wien.*, **61**, 367 (1870).
20. Mathur, G. P., and G. Thodos, *AIChE J.*, **11**, 613 (1965).

Manuscript received August 28, 1967; revision received May 24, 1968; paper accepted June 14, 1968.

Temperature Gradients in Turbulent Gas Streams:

Investigation of the Limiting Value of Total Prandtl Number

WU-SUN CHIA and B. H. SAGE
California Institute of Technology, Pasadena, California

Measurements of the total viscosity and total conductivity were made as a function of position and Reynolds number for the flow of air between two parallel plates with a separation of approximately 0.7 in. The temperature of the upper plate was 130.0°F. and that of the lower plate 70.0°F. The investigations were carried out at Reynolds numbers from 40,000 to 100,000 and were in good agreement with earlier data obtained at Reynolds numbers up to 40,000. The results obtained indicate little change in the total Prandtl number with increasing Reynolds number from the value of the molecular Prandtl number.

An understanding of the interrelation of momentum and energy transport in turbulent flow is a matter of engineering interest. A great deal of effort has been directed to the measurement of momentum transfer from knowledge of local values of velocity and shear. More limited investigations have been carried out in the field of thermal transfer. The experimental techniques in the field of thermal transfer are often simpler and may permit a more accurate evaluation of such transport phenomena than can be obtained readily from the measurements of momentum transfer. The solution of the equations representing the energy balance in a turbulent stream can be readily determined for a variety of conditions (*15, 27*), provided local values of thermal transport are available.

Reynolds (*26*) and Prandtl (*25*) indicated the basic characteristics of convective thermal transfer when treated as directly analogous to momentum transfer. The work of von Karman (*17*) outlined the principal relationships associated with the concepts of eddy viscosity and eddy conductivity which afford a useful, although empirical, tool in the evaluation of the effect of turbulence upon the transfer of momentum and energy. Boelter and co-workers (*3*) extended the Reynolds analogy (*26*) and the concepts of von Karman (*17*), and utilized such approaches to predict the thermal transfer to fluids flowing in conduits. More recent studies (*8, 13, 22, 24, 27*) have determined more fully the effect of Reynolds number and position in the flow channel upon the values of the eddy viscosity and the eddy conductivity for a steady, nearly uniform flow of air between parallel plates.

ANALYTICAL RELATIONS

von Karman (*17*) defined eddy viscosity for steady,